Pergamon

Journal of Structural Geology, Vol. 17, No. 11, pp. 1579 to 1585, 1995

0191-8141/95 $9.50+0.00

0191-8141(95)00045-3

Restraining step behaviour along the Nobi fault system, central Japan

XIWEI XU* and NOBUYUKI YONEKURA

Department of Geography, University of Tokyo, Tokyo 113, Japan

(*Received* 24 *October* 1994; *accepted in revised form* 10 *April* 1995)

Abstract—The Nobi fault system consists of en-échelon left-lateral strike-slip faults. Two restraining steps, the Midori and Hakusan upwarps, have formed between the en-échelon faults, and have demonstrated different failure behaviour. The Midori upwarp has developed into a secondary reverse fault while the Hakusan one has not and is still a fold. Structurally, the Midori upwarp is more evolved than the Hakusan upwarp. Recent faulting has had a shorter recurrence interval since c. 14 ka B.P. This change may have been associated with the development of the secondary reverse fault through the Midori upwarp, as an effective linkage in the Nobi fault system.

INTRODUCTION

Strike-slip fault systems often consist of numerous discrete faults (Segall & Pollard 1980). Releasing (pull-apart basin) and restraining (pressure-ridge) steps are two fundamental types of structures that separate these discrete faults (Sylvester 1988). No matter how large such steps are, they are apparently not permanent and fail eventually at a certain evolutionary stage (Wesnousky 1988, Susong *et al.* 1990, Sylvester 1988). Both geological and geophysical evidence indicates that secondary normal or strike-slip faults may, under appropriate conditions, occur within the releasing steps to link the discrete strike-slip faults (Segall & Pollard 1980, Rodgers 1980, Aydin & Nur 1982, Mann *et al.* 1983). Observation of the 1920 Haiyuan earthquake ruptures (M = 8.6) at the northeastern margin of the Tibetan Plateau shows that a secondary strike-slip fault with a component of dip-slip motion developed as a transfer zone that obliquely bisected the Salt Lake Basin (a pull-apart basin) along the active fault zone (Burchfiel *et al.* 1991). Mechanical analysis of faulting on the basis of two-dimensional and elastic models suggests that antithetic shear faults might occur within the restraining step (McGarr *et al.* 1979, Segall & Pollard 1980). Several authors have also mentioned the structure of pressure-ridges such as Ocotillo Badlands along the Coyote Creek fault in southern California, on which the Pleistocene sedimentary strata are warped into an anticlinal dome with a topographic relief of 200 m above the surrounding desert (Sharp & Clark 1972, Brown & Sibson 1989). However, no case studies have been presented to address the faulting behaviour at a restraining step or pressure-ridge.

This paper mainly discusses the structural contrast between two restraining steps located at Mt. Hakusan and Midori along the Nobi fault system. We also examine failure behaviour in successive events and associated paleoseismicity.

STRUCTURAL GEOLOGY OF THE NOBI FAULT SYSTEM

The Nobi fault system is one of the most active fault systems in central Japan and its horizontal left-slip rate has averaged 2 mm/yr during the past 15,000 yrs (Research Group for Active Faults 1991, Okada *et al.* 1992). It consists of numerous en-échelon left-lateral strike-slip faults. From the northwest to the southeast, they are the Nukumi, Neodani, Midori and Umehara faults respectively (Fig. 1). A pressure-ridge about 3 km wide and 4 km long, named as Hakusan upwarp, has formed in the restraining step between the Nukumi and Neodani faults. Mt. Hakusan is the highest peak in this region with an altitude of 1617 m above sea level and is mainly composed of Mesozoic granite. To the south at Midori, a small pressure-ridge 0.5 km wide is developed in the restraining step between the Neodani and Midori faults. Geomorphologically, the pressure-ridge at Midori has the form of a triangular upwarp, named as the Midori upwarp, which is composed of Mesozoic mudstone. The Daishogun fault is a secondary reverse fault developed within the Midori upwarp. Although no pull-apart basin has developed yet in the 2.1 km wide and 4 km long releasing step between the Midori and Umehara faults, the bedrock elevation is several tens of meters lower than the surrounding areas, reflecting the subsidence that has occurred within this releasing step.

CHARACTERISTICS OF THE RESTRAINING STEPS

Two restraining steps, the Midori and Hakusan upwarps, are well developed along the Nobi fault system. Geological mapping indicates that the Nobi fault

*Permanent address and correspondence to: Xiwei Xu, Institute of Geology, State Seismological Bureau, Beijing 100029, China.

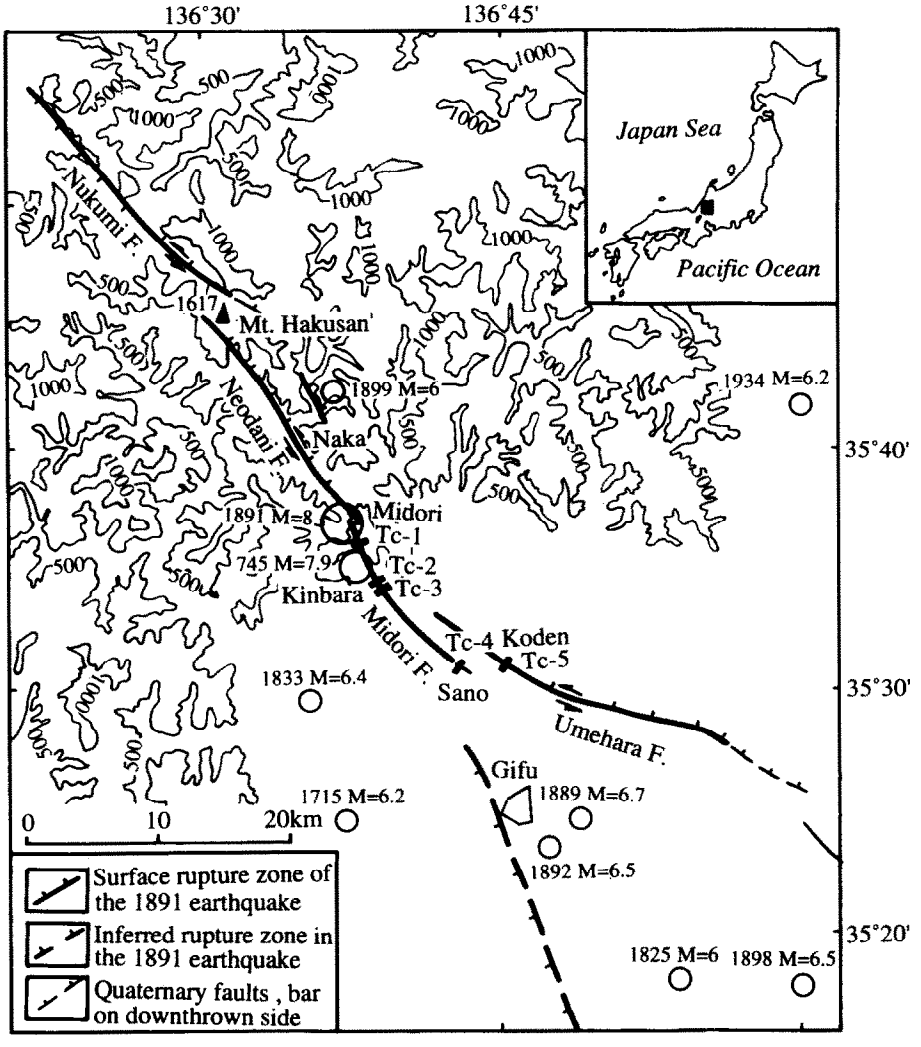

Fig. 1. Distribution of active faults and large historical earthquakes along the Nobi fault system. Shaded rectangle in inset map at the right upper corner shows the location of this figure in Japan. The solid rectangles, labelled Tc-1, 2, 3, 4, 5, across the different fault sections represent locations of excavated trenches. Corresponding references are listed in Table 1.

system was ruptured and both the steps failed to stop the rupture propagation during the 1891 Nobi earthquake (M = 8, Matsuda 1974). The ruptures were about 17 km long on the Nukumi fault, 20 km on the Neodani fault, 11 km on the Midori fault and 23 km on the Umehara fault (fig. 1, Research Group for Active Faults 1991). The largest horizontal displacement reached 3 m on the Nukumi fault, 6–9.2 m on the southeastern section of the Neodani fault, 4–5.6 m on the northwestern section of the Midori fault near the Midori upwarp and 5 m on the Umehara fault (Fig. 2). Generally, the vertical separation reached 2–3 m on those faults, reflecting uplift of the southwestern side of the Nobi fault system during the 1891 earthquake. The maximum vertical (reverse) separation reached 6 m on the EW-trending Daishogun fault at the northern margin of the Midori upwarp (Matsuda 1974), reflecting the reverse faulting that occurred on the Daishogun fault (Fig. 2). Data from levelling surveys show a domal upheaval of 1–3 m around Mt. Hakusan (Muramatsu 1976), reflecting a local crustal shortening that occurred through the Hakusan upwarp during the 1891 earthquake. The above rupture pattern demonstrates that two restraining steps have different structural features and failure regimes in geological history.

Midori upwarp

Geomorphological mapping in the Midori upwarp at a scale of 1:2500 indicates that late Quaternary gravel and sand have been deposited over the Paleozoic and Mesozoic bedrock (Fig. 3). Three terraces whose ages increase with elevation above the modern river channel have developed along Neogawa River. The lowest and also youngest terrace (T_1), 2.2–2.7 m high above the stream bed, formed only after the 1891 Nobi earthquake. The T_2 terrace is about 190 ± 75 to 700 ± 93 yrs old. The T_3 terrace formed about 14,470 ± 200 yrs B.P. (Okada & Matsuda, 1992). These ages are ^{14}C dates from terrace deposits. Both the T_2 and T_3 terraces were strongly deformed or cut by the Daishogun fault, a reverse fault developed within the Midori upwarp, during the 1891 earthquake.

The Daishogun fault within the Midori upwarp connects the ends of the Midori and Neodani faults. It strikes N70°–75°E, dips SSE and is about 500 m long

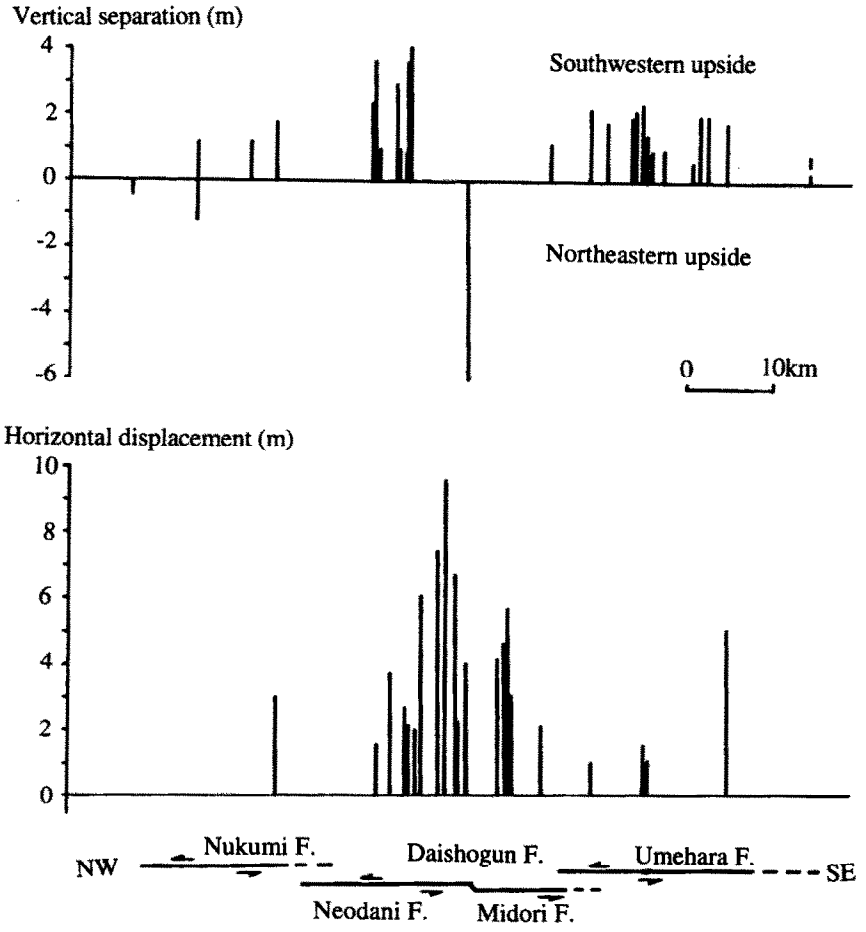

Fig. 2. Distribution of horizontal and vertical displacements of the surface ruptures of the 1891 Nobi earthquake. Data from Hayashi (1971), Matsuda (1974) and Sato *et al.* (1992).

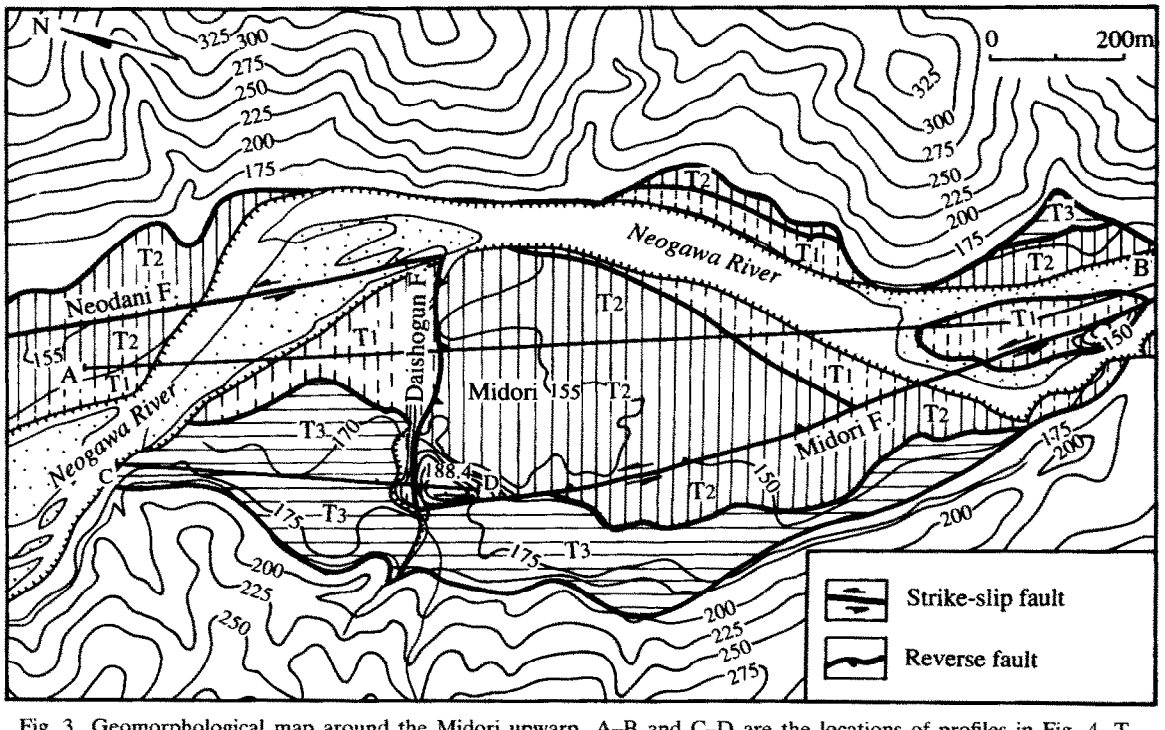

Fig. 3. Geomorphological map around the Midori upwarp. A–B and C–D are the locations of profiles in Fig. 4. T_1 represents the youngest terrace formed after the 1891 earthquake, T_2 the second terrace formed before the 1891 earthquake, and T_3 the third terrace about 14,470 yrs old. Non-ornamented areas are bedrock.

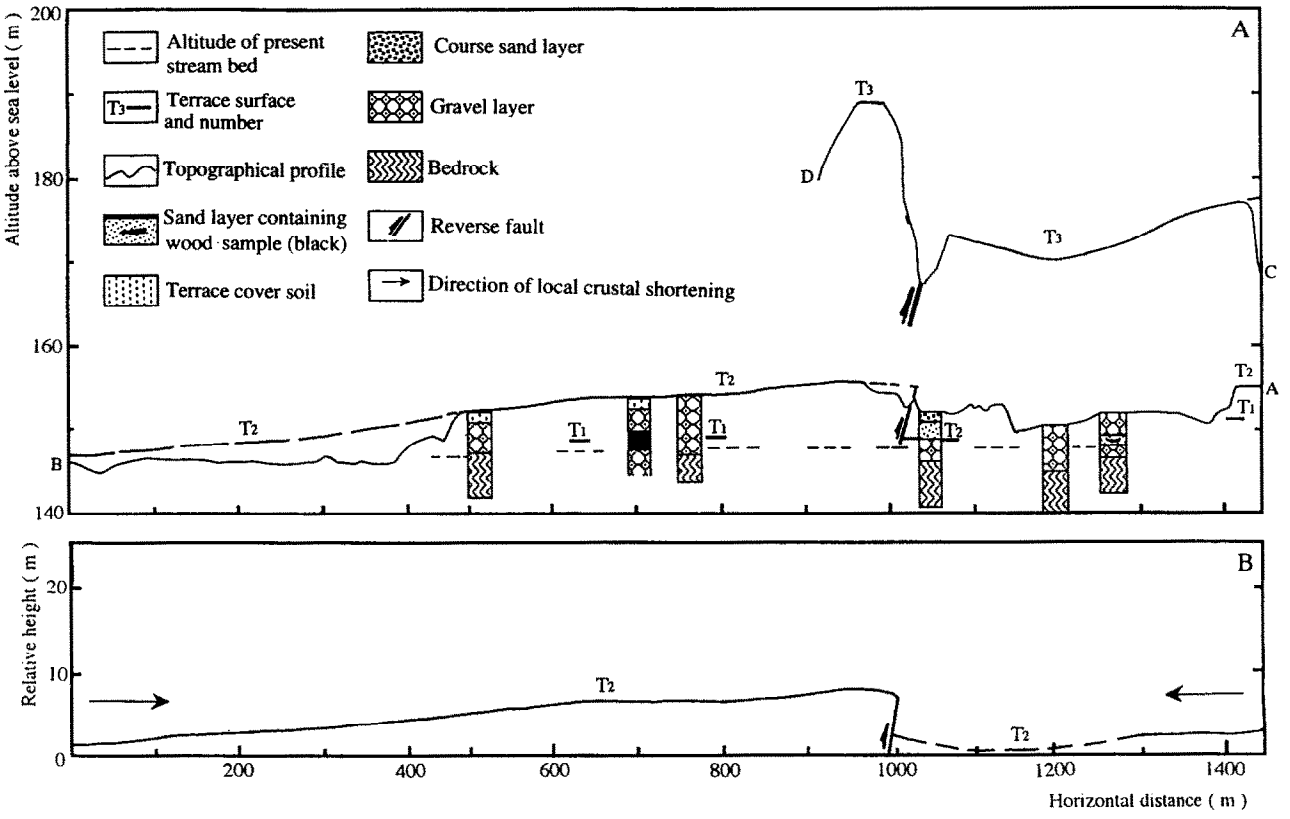

Fig. 4. Topographical profiles across the Midori upwarp along the strike of the fault system (A–B and C–D in Fig. 2). Upper A–B profile shows relative heights of T_1, T_2 and T_3 terrace surfaces; lower profile shows elevation of the T_2 terrace surface relative to the stream bed of the Neogawa River.

(Fig. 3). According to the historical record, the vertical separation along the Daishogun fault in the 1891 earthquake reached 5 ± 1 m (Matsuda 1974). A topographic profile parallel to the strikes of the Midori and Neodani faults within the Midori upwarp (Fig. 4) shows that T_2 terrace surface on the hanging wall of the Daishogun fault has been uplifted and slightly arched near the leading edge. Conversely, the terrace surface has been relatively dropped and downbuckled on the footwall. Thus, in the 1891 earthquake, the main crustal deformation of the Midori upwarp was dip-slip (reverse) rupture on the Daishogun fault and slight fault-propagation bending near the fault plane. The maximum left-lateral horizontal displacement in the 1891 earthquake reached 4.5–5.6 m on the Midori fault and 6–9.2 m on the Neodani fault, respectively (Hayashi 1971, Matsuda 1974), very close to the southeast and northwest of the Midori upwarp (Fig. 2). The amount of crustal shortening within the upwarp thus was in the order of 4.5–9.2 m in the NW–SE direction, consistent with the vertical separation of 5 ± 1 m along the Daishogun fault.

The Daishogun fault has also displaced T_3 terrace with a vertical separation of 14.5 ± 1 m (Fig. 4), of which 5 ± 1 m was generated during the 1891 earthquake. The remaining displacement of about 10 m was generated by two or more events before 1891 AD but after the formation of T_3 terrace at c. 14 ka B.P. During this time period, the total crustal shortening accumulated on the Midori and Neodani faults is 25 ± 3 m (Xu *et al.* 1995). If all of the shortening is accommodated on the Daishogun fault, then its dip can be calculated from the vertical separation of 14.5 ± 1 m. This calculation yields a dip of 30° ± 3°. Evidence for repeated rupture of the Daishogun fault since c. 14 ka B.P. (T_3 terrace age) suggests the reverse motion on this fault has transferred the left-slip motion between the Neodani and Midori faults.

Hakusan upwarp

The 3 km wide sidestep in the Nobi fault system at the Hakusan upwarp also failed to arrest the rupture propagation during the 1891 Nobi earthquake (Figs. 1 and 5). There are no available historical observations to address how the Hakusan upwarp was deformed in the 1891 earthquake, but left-lateral displacements of 1.5–3.5 m occurred on both the Nukumi and Neodani faults near the upwarp (Matsuda 1974). Strong compression must have taken place at the upwarp during the 1891 earthquake to accommodate this left-lateral motion. The amount of crustal shortening within the upwarp thus was in the order of 1.5–3.5 m in the NW–SE direction, consistent with the domal upheaval of 1–3 m around Mt Hakusan (Muramatsu 1976). Topographic profiles show that the Hakusan upwarp exists only within the step between the two faults, and is represented by an anticlinal dome with a topographic relief of 400–600 m above the surrounding areas (Figs. 5 and 6). This relief must have accumulated during many episodes of slip associated with the left-slip motion on both the Neodani and

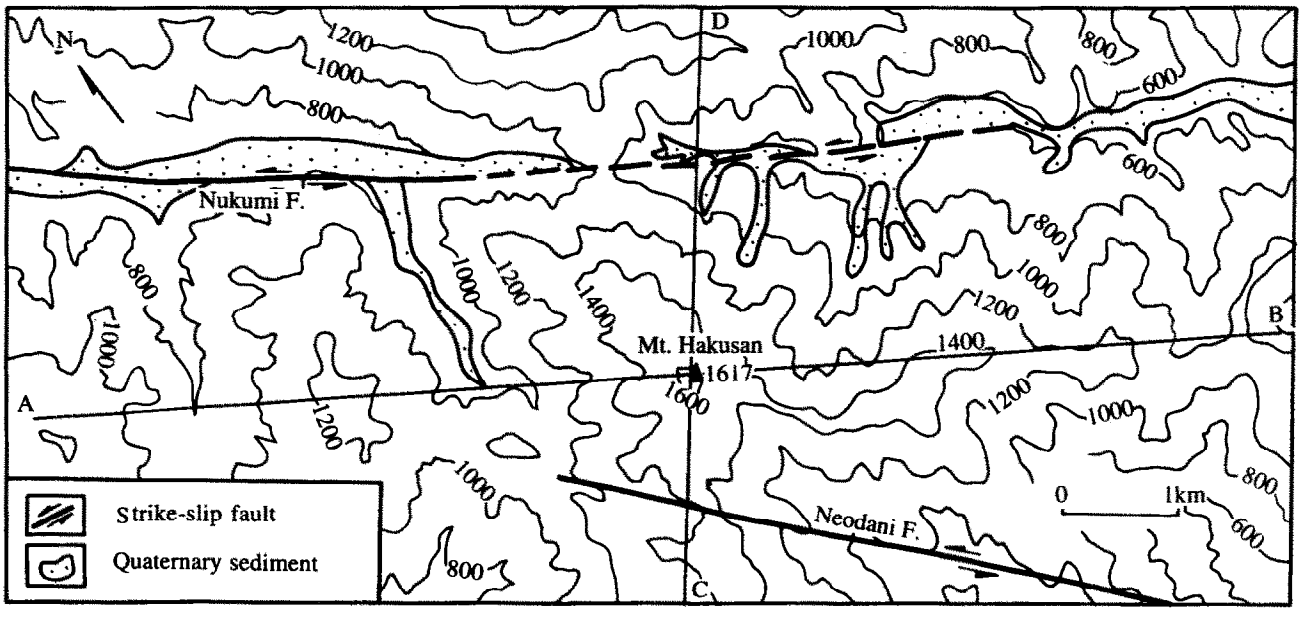

Fig. 5. Geomorphological map around the Hakusan upwarp. A–B and C–D are the locations of profiles in Fig. 6.

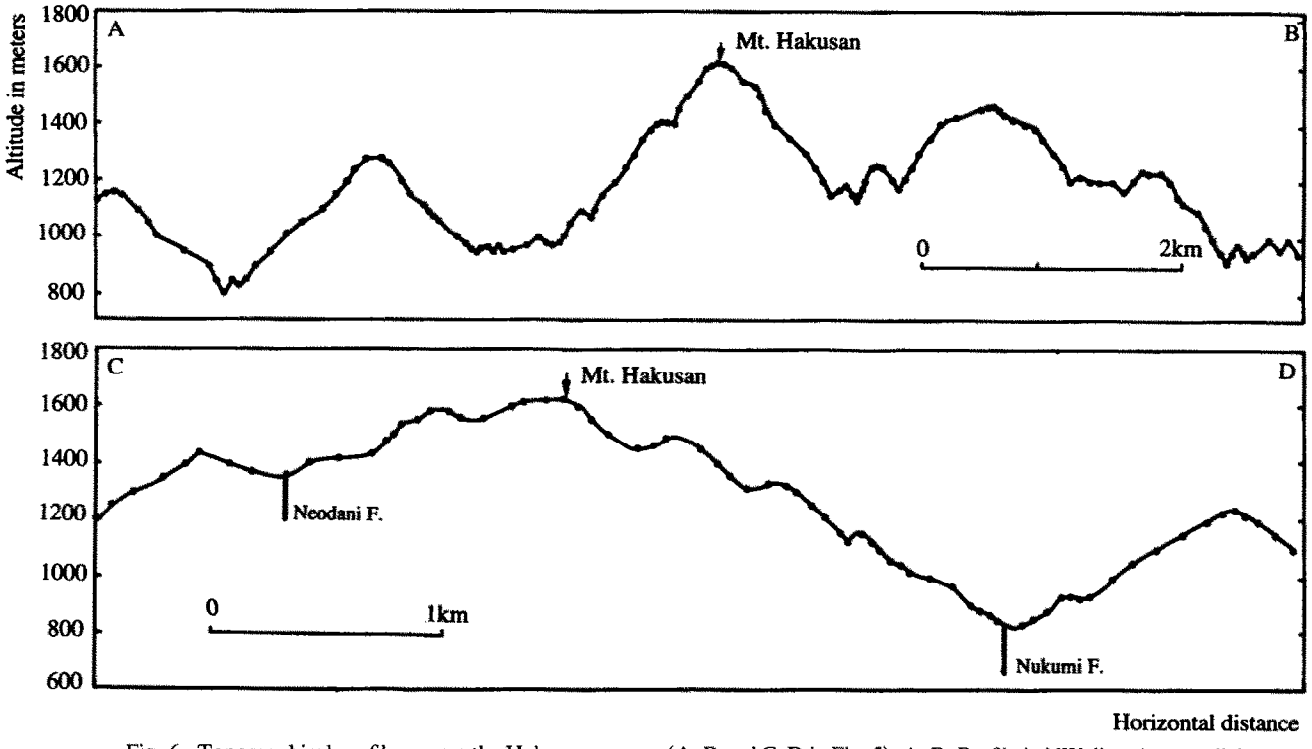

Fig. 6. Topographical profiles across the Hakusan upwarp (A–B and C–D in Fig. 5); A–B: Profile in NW direction parallel to the Nukumi and Neodami fault; C–D: Profile in NE direction across the Hakusan upwarp.

Nukumi faults. No reverse faults have ruptured through the upwarp as is the case with the Midori upwarp, and presumably the fold has accommodated the transfer of left-slip motion between the two parallel strike-slip faults.

Thus, the Midori and Hakusan upwarps are mostly characterized by reverse faulting and fold-related uplift, respectively, and hence are at different evolutionary stages. A reverse fault, the Daishogun fault, has developed within the Midori upwarp to connect the strike-slip faults and most of the local crustal shortening is transferred to thrusting on this reverse fault. No reverse fault has yet propagated to the surface on the Hakusan upwarp and most of the crustal shortening is primarily taken up by folding. The difference in failure behavior of the two upwarps in accommodating left-slip motion of strike-slip faults may be related to the step size and total strain. Results from numerical analysis on the effect of fault interaction at restraining steps indicates that fault propagation energy for closely spaced en-échelon faults increases as the inner fault tips approach each other (Aydin & Schultz 1989), and this implies that a smaller

Table 1. Paleoearthquake data on the Nobi fault system

Trench No.	Location	Event Ages (yrs B.P.)	References
Tc–1	Koden (Umehara F.)	a. 1891 AD (ruptured b. 20000* c. 28000* d–f. >30000	Okada *et al.* 1992
Tc–2	Kinbara (Midori F.)	a. 1981 AD b. 1210 ± 100-1870 ± 150 c. 1870 ± 150-5930 ± 170 d. 10380 ± 290-20000 e. >20000	Miyakoshi *et al.* 1988
Tc–3	Kinbara (Midori F.)	a. 1891 AD b–d. No age data	Kumamoto *et al.* 1992
Tc–4	Midori (Midori F.)	a. 1891 AD ?	Sato *et al.* 1992

*Indicates that event age is close to this value. No events are revealed in the trench (Tc–5) excavated at Sano (location is shown in Fig. 1).

step will undergo stronger deformation and will more easily be broken during large strike-slip earthquakes than a larger one (Barka & Kadinsky-Cade 1989).

The Hakusan upwarp is far larger than the Midori upwarp, suggesting that it can accommodate far greater left-slip motion on the associated strike-slip faults through folding and uplift. Field observation of fault geometry shows that the number of steps per unit length along the trace of major strike-slip fault zones is a smoothly decreasing function of cumulative geological offset (Wesnousky 1988), suggesting a limited total strain that a step can undergo before it breaks and disappears. Supposing that most of the left-slip motion on strike-slip faults are transferred to local crustal shortening at the restraining step by compressional structures, the rupture pattern of the 1891 earthquake indicates that the compressional strain within the Midori upwarp should be greater than that within the Hakusan upwarp. If the long-term faulting behavior of the Nobi fault system follows a characteristic model and the cumulative slip pattern is similar to that of the 1891 earthquake ruptures (Schwartz & Coppersmith 1984, Schwartz 1989), the total compressional strain (crustal shortening) that has been absorbed within the Midori upwarp should be also greater than that within the Hakusan upwarp since their initiation. Structurally, the Midori upwarp is more evolved than the Hakusan upwarp, because the Midori upwarp has developed into a secondary reverse fault perpendicular to the strike-slip faults while the Hakusan one has not and is still a fold.

PALEOSEISMICITY

We consider that the development of secondary reverse faults within a restraining step is an important geological stage during the structural evolutionary process of linking discrete strike-slip faults and present some paleoseismicity in support of this idea. Five large trenches have been excavated on the Nobi fault system since 1981 (Disaster Prevention Research Institute 1983 & 1986, Miyakoshi *et al.* 1988, Kumamoto *et al.* 1992, Okada *et al.* 1992, Sato *et al.* 1992). One of them is located on the Umehara fault (Tc–5), and others are on the Midori fault (Tc–1, 2, 3, 4 in Fig. 1 and Table 1). Paleoseismic data from the Tc–5 trench shows that the Umehara fault had a relatively independent history of surface rupturing earthquakes before 1891 AD, with recurrence intervals longer than 8000 yrs (Okada *et al.* 1992).

Paleoseismic data shows that the Neodani, Daishogun and Midori faults have had very similar faulting histories, with three or four rupture events since the formation of the T_3 terrace (c.14 ka B.P.). The horizontal offset in this time has reached 28 m at Naka village on the Neodani fault where 6–9.2 m horizontal displacement occurred during the 1891 earthquake. Vertical separation has reached 14.5 m on the Daishogun fault where 5 ± 1 m vertical separation occurred during the 1891 earthquake. Supposing that the surface-rupturing earthquakes are characteristic, we can infer that three or four earthquakes have taken place on these three faults since 14,470 yrs B.P. From the Tc–2 trench excavated at Kinbara on the Midori fault (Miyakoshi *et al.* 1988), it is known that the latest one is the 1891 Nobi earthquake (M = 8) which ruptured the entire fault system; the second event took place in 745 AD (M = 7.9, Usami 1987), the third event occurred between 5930 and 1870 yrs B.P., and the fourth event occurred between 10,380 and 20,000 yrs B.P. Still older events probably occurred prior to 20,000 yrs (Table 1). The recurrence interval between these events appears to become shorter closer to the present, and ranges from more than 10,000–1150 yrs. The intervals of the recent three events which generated surface ruptures simultaneously on the Midori, Neodami and Daishogun faults, vary from 4720 to 1150 yrs, much shorter than the previous interval on the linked section (Midori, Neodani and Daishogun faults) or that of the Umehara fault. Since the Daishogun fault has moved during the latest three events, we infer that the recent faulting process, at a shorter recurrence interval since c. 14 ka B.P., may have been associated with the development of the Daishogun fault through the Midori upwarp, as an effective linkage in the Nobi fault system. Additionally, if every paleoearthquake in the last 20 ka generated a similar surface

rupture pattern to that of the 1891 earthquake, at least on the Neodani, Daishogun and Midori faults, the amount of crustal shortening may have reached 27.6 ± 9.6 m through the Midori upwarp and about 10 ± 4 m during the last four events.

CONCLUSIONS

A reverse fault, the Daishogun fault, has ruptured through the Midori upwarp. This fault is nearly perpendicular to the discrete parallel strike-slip faults, and dips at about 30° ± 3°. The strike-slip motion on the Midori and Neodani faults is transferred into reverse motion on the Daishogun fault. Faults have not ruptured through the Hakusan upwarp and the strike-slip motion on the Neodani and Nukumi faults is transferred by folding deformation in the Hakusan upwarp.

Linkage between fault sections has enabled most of the fault segments within the Nobi fault system to rupture in at least the last three events on the Nobi fault system, including the 1891 Nobi earthquake. In addition to enhancing the potential for through-going rupture, the linkage of faults appears to have facilitated more frequent rupture of the fault system.

Acknowledgements—The authors are very grateful to Prof. Atsumasa Okada of Kyoto University, Japan, for provision of his original scientific data, from which we benefited greatly in preparing this paper. The first author acknowledges the support of the Japan Society for the Promotion of Science (JSPS) under the Post-doctoral Fellowship Program for Foreign Researchers.

REFERENCES

Aydin, A. & Nur, A. 1982. Evolution of pull-apart basins and their scale independence. *Tectonics* **1**, 91–105.

Aydin, A. & Schultz, R. A. 1989. The effect of fault interaction on the stability of echelon strike-slip faults. *U.S. Geol. Surv. Open-File Report* **89–315**, 47–66.

Barka, A. A. & Kadinsky-Cade, K. 1989. Effects of restraining stepovers on earthquake rupture. *U.S. Geol. Surv. Open-File Report* **89–315**, 67–79.

Brown, N. N. & Sibson, R. H. 1989. Structural geology of the Ocotillo badlands antidilational fault jog, southern California. *U.S. Geol. Surv. Open-File Report* **89–315**, 94–109.

Burchfiel, B. C., Zhang, P., Wang, Y., Zhang, W., Song, F., Deng, Q., Molnar, P. & Royden, L. 1991. Geology of the Haiyuan fault zone, Ningxia-Hui Autonomous Region, China, and its relation to the evolution of the northeastern margin of the Tibetan Plateau. *Tectonics*, **10**, 1091–1110.

Disaster Prevention Research Institute 1983. Trench across the trace of the 1891 Nobi earthquake faults. *Report of the Coordinating Committee for Earthquake Prediction* **29**, 360–367 (in Japanese)

Disaster Prevention Research Institute 1986. Trench survey at Sano in 1981 on the Neodani fault, Nobi active fault system. *Active Fault Research*, **3**, 33–36 (in Japanese)

Hayashi, N. 1971. The horizontal displacements at Naka village on the Neodani fault. *Review of Geography*, **44**, 875–877 (in Japanese)

Kumamoto, T., Okada, A., Onda, S., Uyeda, K. & Ikeda, Y. 1992. Trench survey in 1991 at Kinbara on Neodani fault, Nobi fault system. *Active Fault Research*, **10**, 85–91 (in Japanese)

Mann, W. P., Hempton, M. R., Bradley, D. C. & Burke, K. 1983. Development of pull-apart basins. *J. Geol.* **91**, 529–554.

Matsuda, T. 1974. Earthquake fault of the 1891 Nobi earthquake. *Bull. Earthquake Res. Inst. Univ. Tokyo* **13**, 85–126 (in Japanese)

McGarr, A., Pollard, D. D., Gay, N. C. & Ortlepp, W. D. 1979. Observations and analysis of structures in exhumed mine-induced faults. In: *Proceedings of Conference VIII: Analysis of Actual Fault Zones in Bedrock, U. S. Geol. Surv. Open File Rep.* **79–1239**, 101–120.

Miyakoshi, K., Ogata, S., Kakuda, T., Satake, Y., Tanaka, K., Kiho, K., Inohara, Y. & Kanaori Y. 1988. Activity of the Neodani fault — characteristics and analysis of fault movement at Kinbara, Gifu Prefurture. *Abiko Res. Laboratory Rep.* **U88052**, 1–37 (in Japanese)

Muramatsu, K. 1976. Neodami fault and Nobi earthquake. *Geol. Review, Japan*, **12**, 117–127 (in Japanese)

Okada, A. & Matsuda, T. 1992. Late Quaternary activity of the Neodami (Neo-Vally) fault at Midori and Naka, Neo village, central Japan. *J. Geography*, **101**, 19–37 (in Japanese)

Okada, A., Watanabe, M., Ando, M., Tsukuda, T. & Hirano, S. 1992. Estimation of paleo-seismicity in the Nobi active fault system. Central Japan — excavation study of the Umehara fault, central strand in the Nobi active fault system. *J. Geography* **101**, 1–18 (in Japanese)

Research Group for Active Faults 1991. *Active Faults in Japan: Sheet Maps and Inventories (revised edition)*. Univ. Tokyo Press, Tokyo.

Rodgers, D. A. 1980. Analysis of basin development produced by en-echelon strike slip faults. In: *Sedimentation at Oblique-Slip Margins* (edited by Ballance, P. F. & Reading, H. G.). *Spec. Publs. Int. Ass. Sedim.* **4**, 27–41.

Sato, H., Okada, A., Matsuda, T. & Kumamoto, T. 1992. Geology of a trench across the Midori fault scarp, from the 1891 Nobi earthquake, central Japan. *J. Geography*, **101**, 556–572 (in Japanese)

Schwartz, D. P. 1989. Paleoseismicity, persistence of segments, and temporal clustering of large earthquakes – examples from the San Andreas, Wasatch, and Lost River fault zone. *U. S. Geol. Surv. Open-File Report* **89–315**, 361–375.

Schwartz, D. P. & Coppersmith K. J. 1984. Fault behavior and characteristic earthquakes: examples from the Wasatch and San Andreas fault zones. *J. Geophys, Res.* **89**, 5681–5698.

Segall, P. & Pollard, D. D. 1980. Mechanics of discontinuous faults. *J. Geophys. Res.* **85**, 4337–4350.

Sharp, R. V. & Clark, M. M. 1972. Geologic evidence of previous faulting near the 1968 rupture on the Coyote Creek fault. *U. S. Geol. Surv. Prof. Pap.* **787**, 131–140.

Sibson, R. H. 1989. Earthquake faulting as a structural process. *J. Struct. Geol.* **11**, 1–14.

Susong, D. D., Janecke, S. U. & Bruhn, R. 1990. Structure of a fault segment boundary in the Lost River fault zone, Idaho, and possible effect on the 1983 Borah Peak earthquake rupture. *Bull. Seism. Soc. Am.* **80**, 57–68.

Sylvester, A. G. 1988. Strike-slip faults. *Bull. Geol. Soc. Am.* **100**, 1666–1703.

Xu, X., Yonekura, N. & Suzuki, Y. 1995. Kinematics and Geometry of the Midori-Daishogun fault along the Nobi fault system, Central Japan. *J. Geography*, (in press)

Usami, T. 1987. *The Catalogue of Disaster Earthquakes in Japan* (revised edition). Univ. Tokyo Press, Tokyo.

Wesnousky, S. G. 1988. Seismological and structural evolution of strike-slip faults. *Nature* **335**, 340–342.